



Accurate Fruits Fault Detection in Agricultural Products Using an Efficient Algorithm

Hamidreza Saberhari

Received: 24 August 2015,

Accepted: 03 October 2015

Abstract

The main purpose of this paper was to introduce an efficient algorithm for fault identification in fruits images. First, input image was de-noised using the combination of Block Matching and 3D filtering (BM3D) and Principle Component Analysis (PCA) model. Afterward, in order to reduce the size of images and increase the execution speed, refined Discrete Cosine Transform (DCT) algorithm was utilized. Finally, for segmentation, fuzzy clustering algorithm with spatial information was applied on the compressed image. Implementation results in MATLAB environment and based on the gathered data showed that the proposed algorithm contains a good capability in de-noising. Also, in the proposed method, identification accuracy of faulty regions in fruit was higher than other methods. The major advantage of the proposed method was its high speed which makes it appropriate for real time applications.

Keywords:

Fault, DCT transform, Noise, Image processing

INTRODUCTION

In recent decades, image processing systems have been used in order to automatically control many processes and analyze them in different fields such as food, agriculture, and pharmacy and textile industry. Among them, one of the most popular applications of image processing and machine vision is the quality inspection of agricultural products such as fruits and vegetables based on shape, color, and the fault in them (Arumugam *et al.*, 2011). For judging the quality of this type of agricultural products, machine vision systems use digital cameras to take images, and then these images are analyzed through image processing systems (Abbot, 1999).

Among variety of agricultural products, apple suffers from so many faults. This fruit contains so many changes in skin color. Based on the market standard published by the European commission, apple quality depends on the size, color, shape and presence/absence of fault in it (Izadbakhshi and Javadikia, 2014). Traditionally, spoiled fruits are separated from high definition ones by manpower, which is very tedious and time-consuming (Malamas *et al.*, 2003). Thus, mechanizing this process using image processing systems leads to increase the identification speed and in the same time, error cancelation and accuracy growth (Brosnan and Sun, 2002; Graves and Batchelor, 2003). Identifying healthy fruits from faulty ones faces major challenges, which some of them are (Hills, 1995; Halls *et al.*, 1998):

- Lighting conditions when imaging the fruit: Create shadow or lighting spots on the fruit due to glossy surface of fruits,
- Inappropriate background for the fruit when imaging: If the background has different colors or the same color as the fruit, fruit identification and also finding faulty regions becomes difficult,
- Different fruits in one image: In an image containing different fruits with different colors, finding fruits from the background gets difficult. For this reason, this condition is considered that there must be just a single type of fruit, and
- Appearance change of some fruits: This problem causes different distributions of color in different spots of the fruit, which causes problem while extracting feature out of it.

A variety of algorithms is proposed for fruit fault identification in references. (Linker *et al.*, 2012) proposed an algorithm to estimate the number of apples in color images of gardens under natural light which consists of four min steps; identifying pixels that belong to apples with high probability, using color and smoothness, forming and developing core areas which are interconnected sets belonging to apples with high probability, and partitioning these seed areas into disordered parts and arcs, and combining these arcs and comparing the obtained circles with a simple model of an apple. Although the algorithm correctly detects more than 85 percent of visible apples in images, straight light and color saturation leads to so many positive detections. (Payne *et al.*, 2013) proposed a method to estimate mango crop using image analysis. This method is for counting mango from daily images of individual trees for machine vision goals based on estimating the mango tree crops. Images of mango trees are taken in a three-day period, three weeks before the commercial harvest. Fruits of one of each 15 trees are counted manual, and these trees are imaged from four sides. Correlation between number of trees and manual counting is strong (for two sides). Five hundred fifty five trees are imaged from one side. In these images, pixels are partitioned using color partitioning in RGB color space and YCbCr color space. The obtained pallets have been counted to achieve the number of mangos in images. Algorithm efficiency reduces with increasing the number of fruits of tree and when imaging in terms of direct sunlight. (Mizushima and Lu, 2013) presented a segmentation method to arrange apples and classify it using Otsu method and support vector machine (SVM) classifier. This method consists of three sections; color separation using linear SVM, color image transformation into gray-scale and automatic and adjustable segmentation using Otsu algorithm. This method requires the minimum number of training data. Also it prevents challenges that fruit color and light conditions changes can bring. (Ramano *et al.*, 2012) applied laser light and digital images combination to estimate the moist content and color in sweet pepper. Optical devices are increasingly used for more accuracy and

faster access when monitoring the quality of agricultural products. The main work done by is evaluation using charge-coupled device (CCD) camera along with light-emitting diode (LEDs) which their radiation wavelength is 532 nm and 632 nm, respectively. So the changes in moist content of green, yellow and red sweet pepper can be analyzed during the drying process. Results show that diffusion area and light intensity have the ability to predict moist content of sweet pepper during drying. In addition, light diffusion changes in accordance with different depths in the surface that the picture is taken. Also the result that a change in tissue structure may make photons scatter over the surface and change distribution levels was achieved. (Moradi *et al.*, 2011) used the statistical histogram based on fuzzy-C means (FCM) to identify fault of apple. First, the input image is transformed from RGB workspace into workspace. After that, shape of the fruit is extracted by active contour model (ACM). Finally, the image is partitioned by SHFCM algorithm. Experimental results displays that FCM and SHFCM have equal number of repeat times to complete the process of partitioning and their results are the same. However, proposed SHFCM algorithm has a higher speed than the standard FCM. The accuracy of the proposed algorithm about resulting images for FCM and SHFCM are 91 percent and 96 percent for intact pixels and defective pixels, respectively. But the problem of this algorithm is its high computation complexity because of using active contour model, and an optimal algorithm is required to minimize energy in active contour model. In the other work done by (Moradi *et al.*, 2012),

expectation-maximization (EM) segmentation algorithm is used for fault identification in apple. In this method, the input image is transformed from RGB workspace into workspace. Then, fruit shape is extracted by ACM. Eventually, image is partitioned by SHEM algorithm. Results indicate that EM and SHEM show pretty equal performances with equal repeats. The discussed SHEM algorithm spends less time than standard EM algorithm. The accuracy of the proposed algorithm for EM and SHEM are respectively 91.72 percent and 94.86 percent for intact pixels and defective pixels (Rakun *et al.*, 2011).

In this paper, an optimal algorithm is presented in order to fault identification in fruit images. First, input image is de-noised using black matching and 3D filtering (BM3D) and principle component analysis (PCA) combined model. Then, modified version of discrete cosine transform (DCT) algorithm is used in order to reduce image size and increase speed of the segmentation task. Finally in partitioning stage, we have used the fuzzy clustering algorithm based on the spatial information of neighboring pixels in the compressed image.

The rest of the paper is as follows: In Section 2, materials and methods used in this paper is presented which consist of our proposed algorithm and its different steps. Implementation results consisting of two experimental phases on gathered data by the author is expressed in Section 3. Finally, Section 4 includes the conclusion of the paper.

MATERIALS AND METHODS

Figure 1 shows block diagram of the proposed algorithm. Different steps of the raised algorithm are as follows, which will be explained:

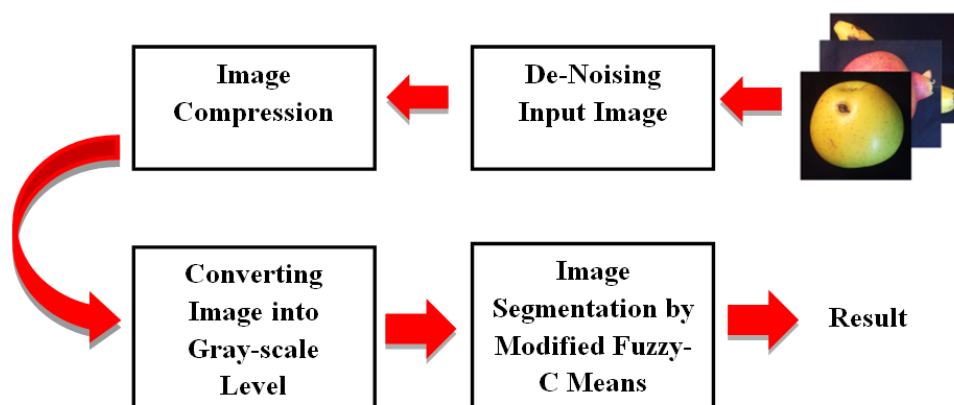


Figure 1: Block diagram of the proposed algorithm

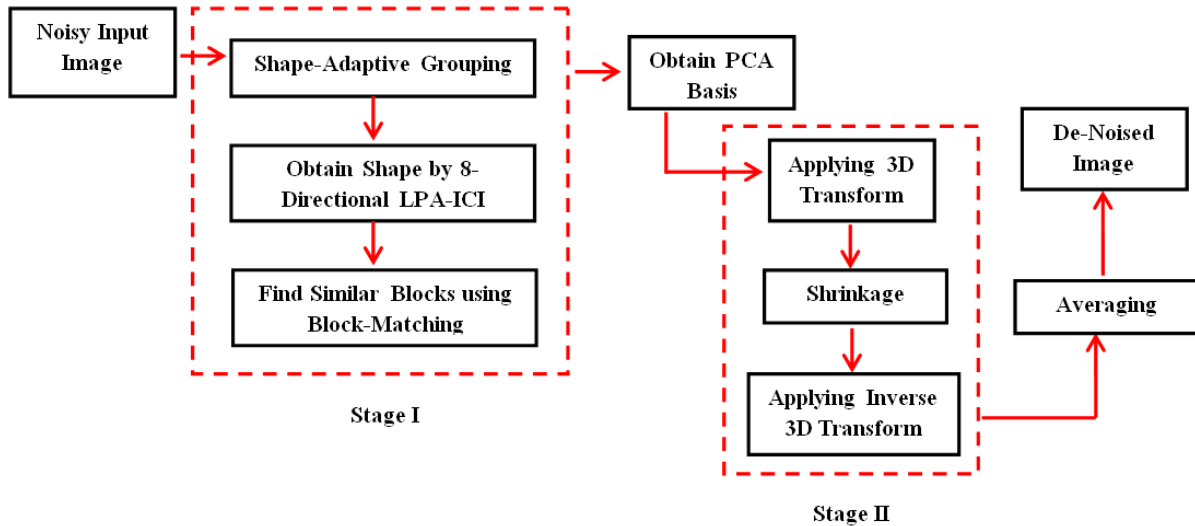


Figure 2: Block diagram of the proposed De-Noising algorithm

- Preprocessing step in order to remove noise using BM3D and PCA combined algorithm,
- Image compression to reduce its size, and
- Fault identification using fuzzy clustering algorithm with spatial data.

Preprocessing stage to De-Noise using BM3D and PCA Combined Algorithm

In the presented algorithm, BM3D and PCA combined model (Dabov *et al.*, 2009) is used to de-noise the image. This model is demonstrated in Figure 2. Assume that the input image is demolished by additive white Gaussian noise with average of zero and variance of σ^2 . The input image is scanned array, and for each processed pixel, the following procedure is applied:

- For each pixel being processed, adaptive-shape neighborhood with the centrality of the pixel can be found using eight-fold LPA-ICI model based on (Foi *et al.*, 2007). The neighborhood is located within a square block of a fixed size. This block is called reference block. The number of pixels in the neighborhood is shown by N_{el} ,
- Blocks similar to the reference block are found using block-matching method and using the method mentioned in the previous step, we extract the adaptive-shape neighborhood from each one of these matching blocks. The number of matching blocks are shown by N_{gr} ,
- Determining a conversion and applying it on adaptive-shape neighborhoods. For this purpose, we consider a threshold level (τ) and

review two states:

1) If the ratio is $N_{gr}/N_{el} \geq \tau$, this means that an acceptable number of neighboring pixels are selected to estimate PCA matrix. Eigenvectors of this matrix form base vectors of PCA. Thus in this step, only eigenvectors (which the eigenvalues corresponding to them are higher than the defined threshold level), are selected.

2) If the ratio is $N_{gr}/N_{el} < \tau$, it means that a sufficient number of similar neighboring pixels are not selected as training data for PCA model. Thus, a certain amount is selected for eigenvector.

- Forming a three-dimensional array by connecting adaptive-shape neighborhoods ($\min N_{gr}, N_2$) with the block reference that has the highest similarity. is a fixed parameter which limits the number of filtered neighborhoods.

- Applying the transformation used in step (3) to each one of adaptive-shape neighborhood groups. In this step, A one-dimensional orthogonal transformation (such as wavelet transformation) is also applied to each one of three-dimensional groups,

- Applying hard-thresholding to three-dimensional spectrum in order to shrinkage the image,

- Applying a three-dimensional reverse transformation from step (5) to find estimations in each of adaptive-shape neighborhood groups, and

- Returning obtained estimations to their original positions using weighed averaging.

Compressing the De-Noised image to reduce its size

The size of the de-noised original image is

3264×1836, which must be compressed. The size of the input image is reduced because it is very high and heavily increases computational cost in the next steps. In this study, in addition to accurately identify faulty areas of fruits, being a real-time system contains a great importance. In this paper, method presented by has been proposed which is based on the improved version of DCT transform to compress de-noised image. DCT transformation is mainly used for compressing signals and images due to energy savings and lack of correlation of samples. More details of this algorithm are explained by (Saberhari and Shamsi, 2012).

Fault identification using fuzzy clustering algorithm with spatial neighboring information

In this paper, fuzzy clustering algorithm (Bezdek, 1987) with spatial information is applied for segmenting the compressed images. Fuzzy clustering algorithm allocates pixels to classes by adapting the fuzzy membership functions. Assume that $X = (x_1, x_2, \dots, x_n)$ is an image with N pixels which belongs to c cluster. Fuzzy clustering algorithm attempts to perform segmentation by minimizing cost function. Cost function in this algorithm is defined as follows:

$$J_m = 2 \sum_{i=1}^c \sum_{k=1}^N (\mu_{ik})^m \|x_k - v_i\|^2 \tag{1}$$

which $V = [v_1, v_2, \dots, v_c]$ is cluster center vector and N is the number of input data. μ_{ij} Shows membership of x_j pixel in i th cluster. Also, m is constant number which controls fuzziness of partitions. In our proposed algorithm, m changes from 1.2 to 5. Euclidean distance norm ($\|\cdot\|$) which is the distance between pixels and average of clusters is achieved as:

$$D_{ik}^2 = \|x_k - v_i\|_{A_D}^2 = (x_k - v_i)^T A_D (x_k - v_i) \tag{2}$$

where A_D is a diagonal matrix defined as:

$$A_D = \begin{bmatrix} \left(\frac{1}{\sigma^2}\right) & 0 & \dots & 0 \\ 0 & \left(\frac{1}{\sigma^2}\right) & \dots & 0 \\ \cdot & \cdot & \cdot & \cdot \\ \cdot & \cdot & \cdot & \cdot \\ \cdot & \cdot & \cdot & \cdot \\ 0 & 0 & \dots & \left(\frac{1}{\sigma^2}\right) \end{bmatrix} \tag{3}$$

The deviation of x_k from v_i can be seen from equation (3). Equation (1) can be rewritten using Lagrange multipliers as follows:

$$J(X; U, V) = \sum_{i=1}^c \sum_{k=1}^N (\mu_{ij})^m D_{ik}^2 + \sum_{k=1}^N \lambda_k \left(\sum_{i=1}^c \mu_{ik} - 1 \right) \tag{4}$$

Considering above equation and the conditions $D_{ik}^2 > 0, \forall i, k$ and $m > 1$, the cost function is minimized. Therefore, the memberships function and cluster center are updated as follows:

$$\begin{aligned} \mu_{ik} &= \frac{1}{\sum_{j=1}^c \left(\frac{D_{ikA}}{D_{jkA}}\right)^{\frac{2}{m-1}}} & 1 \leq i \leq c, 1 \leq k \leq N \\ v_i &= \frac{\sum_{k=1}^N (\mu_{ik})^m x_k}{\sum_{k=1}^N (\mu_{ik})^m} & 1 \leq i \leq c \end{aligned} \tag{5}$$

The above equation displays as weighted average of data points which belong to a cluster, such as weights are the membership matrices.

One of important characteristics of fruit images is high intensity correlation between a pixel and its neighbor pixels. In the other words, these neighboring pixels have similar features; in a way that the probability that a certain pixel belongs to neighboring pixels class is high. Considering the importance of spatial dependence, the need to enter a locative parameter in segmentation algorithms based on intensity appears. Therefore, we enter h_{ij} spatial function into fuzzy clustering algorithm and call it fuzzy clustering algorithm with spatial information (Saberhari et al., 2015).

$$h_{ij} = \sum_{k \in N_{x_j}} \mu_{ik} \tag{6}$$

N_{x_j} indicates a square window with centrality of x_j in spatial field, which in this article a 5×5 window is used. If majority of neighborhoods of a pixel belong to the same class, then, spatial function h_{ij} will be maximum for a central pixel. Implementation process of fuzzy clustering algorithm with spatial data is the same as fuzzy clustering algorithm and its membership function changes as below:

$$\mu'_{ij} = \frac{\mu_{ij}^p h_{ij}^q}{\sum_{k=1}^c \mu_{kj}^p h_{kj}^q} \tag{7}$$

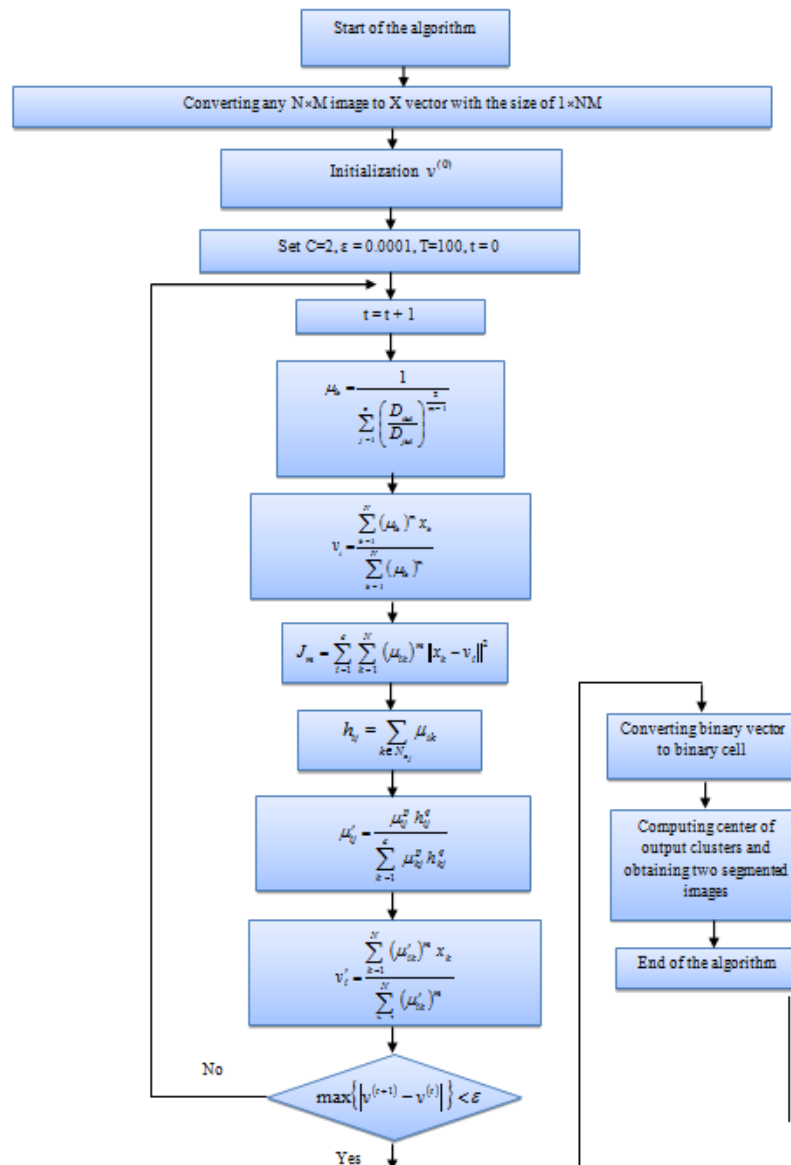


Figure 3: Block diagram of the modified-C means clustering algorithm based on spatial neighboring Information

where p and q are control parameters of both functions. In first step, like fuzzy clustering algorithm, membership functions are computed. In second step, membership function data is mapped into spatial scope and then spatial function is computed out of it. The considerable note is that in homogenous areas spatial function is similar to original membership function. So, clustering result does not change. But for pixels containing noise, the equation above reduces noisy cluster weight by labeling its neighboring pixels. As a result, incorrectly classified pixels are easily corrected from noisy areas. Fuzzy clustering algorithm with spatial data is implemented as the block diagram shown in Figure 3.

RESULTES AND DISCUSSION

Image acquisition device used in this paper is composed of a high resolution (2364×1836 pixels) monochrome digital camera, four interference band pass filters, a frame grabber, a diffusely illuminated tunnel with two different light sources, and a conveyor belt on which fruits are placed. The filters are centered at 450, 500, 750, and 800 nm with the bandwidths of 80, 40, 80, and 50 nm, respectively This device is capable of acquiring only one-view images of fruits. Each of these one-view images was composed of four filter images, which had to be separated by alignment based on pattern matching. All implementation stages of the pro-

posed algorithm are performed on a computer with 3.4 GHz and the RAM memory of 1 GHz.

Experiment I

In the first test, performance of the proposed de-noising algorithm has been compared by the other approaches. For this purpose, the following two criteria have been used for quantitative comparison. Also, some other de-noising algorithms (BM3D, patch based global PCA (PGPCA) and progressive image de-noising (PID) methods proposed by (Charles *et al.*, 2011) and (Knaus and Zwicker, 2014), respectively) have been implemented to compare the results.

Peak signal to noise ratio (PSNR): Peak signal to noise ratio represents the ratio of maximum possible power to noise power. Because many signals have a wide dynamic range, this evaluation criterion arises in the form of logarithm. This criterion is often used to measure the quality of images after reconstruction, the higher the amount of the criterion, the higher the quality of reconstructed image. The signal to noise ratio is defined as the mean square error. If we show the image without noise with I and the noisy image with K, we have (Thu and Ghanbari, 2008):

$$MSE = \frac{1}{mn} \sum_{i=0}^{m-1} \sum_{j=0}^{n-1} [I(i, j) - K(i, j)]^2$$

$$\rightarrow PSNR = 10 \log_{10} \left(\frac{MAX_I^2}{MSE} \right) = 20 \log_{10} \left(\frac{MAX_I}{\sqrt{MSE}} \right) \tag{8}$$

where MAX_I is the maximum possible pixel value, and if image pixels are 8-bit, this value will be 255; otherwise, equation (9) is used to compute MAX_I :

$$MAX_I = 2^B - 1 \tag{9}$$

Structural similarity (SSIM): This criterion is a way to measure the similarity between two images. This criterion is an improved version of previous criterion and the difference is that it considers noises and artifacts in the image as changes in structural information. The structural information is based on the idea that pixels spatially close to each other are greatly dependent on one another and this dependence contains important information. SSIM criterion is defined

based on the following equation:

$$SSIM(x, y) = \frac{(2\mu_x\mu_y + c_1)(2\sigma_{xy} + c_2)}{(\mu_x^2 + \mu_y^2 + c_1)(\sigma_x^2 + \sigma_y^2 + c_2)} \tag{10}$$

where μ_x and μ_y is the average of x and y , σ_x^2 and σ_y^2 is the variance of x and y , respectively. σ_{xy} is the covariance between x and y . c_1 and c_2 are two variables which is defined as, $c_1 = (k_1l)^2$, $c_2 = (k_2l)^2$, respectively. The values of k_1 and k_2 are chosen as 0.01 and 0.03. Also, l is the number of bits of pixel.

In Figures 4, results of applying the proposed de-noising algorithm on input images are given for the different values of standard deviation. As can be seen, noise is greatly removed at all levels of standard deviation.

In Tables 1 and 2, PSNR and SSIM values are given in the proposed de-noising and BM3D-PGPCA and PID algorithms for different standard deviation values. The superiority of the proposed algorithm in improving PSNR and SSIM parameters can be seen in these tables and also in diagrams shown in Figures 5 and 6. For , PSNR quantities are 35.9 and 35.69 in BM3D-PGPCA and PID methods, respectively, while this value is achieved 35.92 in the proposed algorithm. This improvement is also observed for other standard deviations. Similar results were obtained in the SSIM parameter value. By choosing the standard deviation equal to 10, the value of this parameter in the proposed algorithm has improved 5.76 percent and 0.03 percent in comparison to BM3D-PGPCA and PID methods, respectively. There is similar superiority for SSIM parameter in other standard deviation values.

Experiment II

In this test, the performance of our algorithm is compared with other methods in identifying the fruit fault. For this purpose, two following evaluation criteria are utilized. Also two approaches, conventional FCM and Otsu algorithms, are implemented.

Segmentation matching factor (SMF): This parameter measures pixel that have been wrongly segmented and is defined as follows (Ahmed *et al.*, 2002):

Accurate Fruits Fault Detection in Agricultural Products / Saberhari

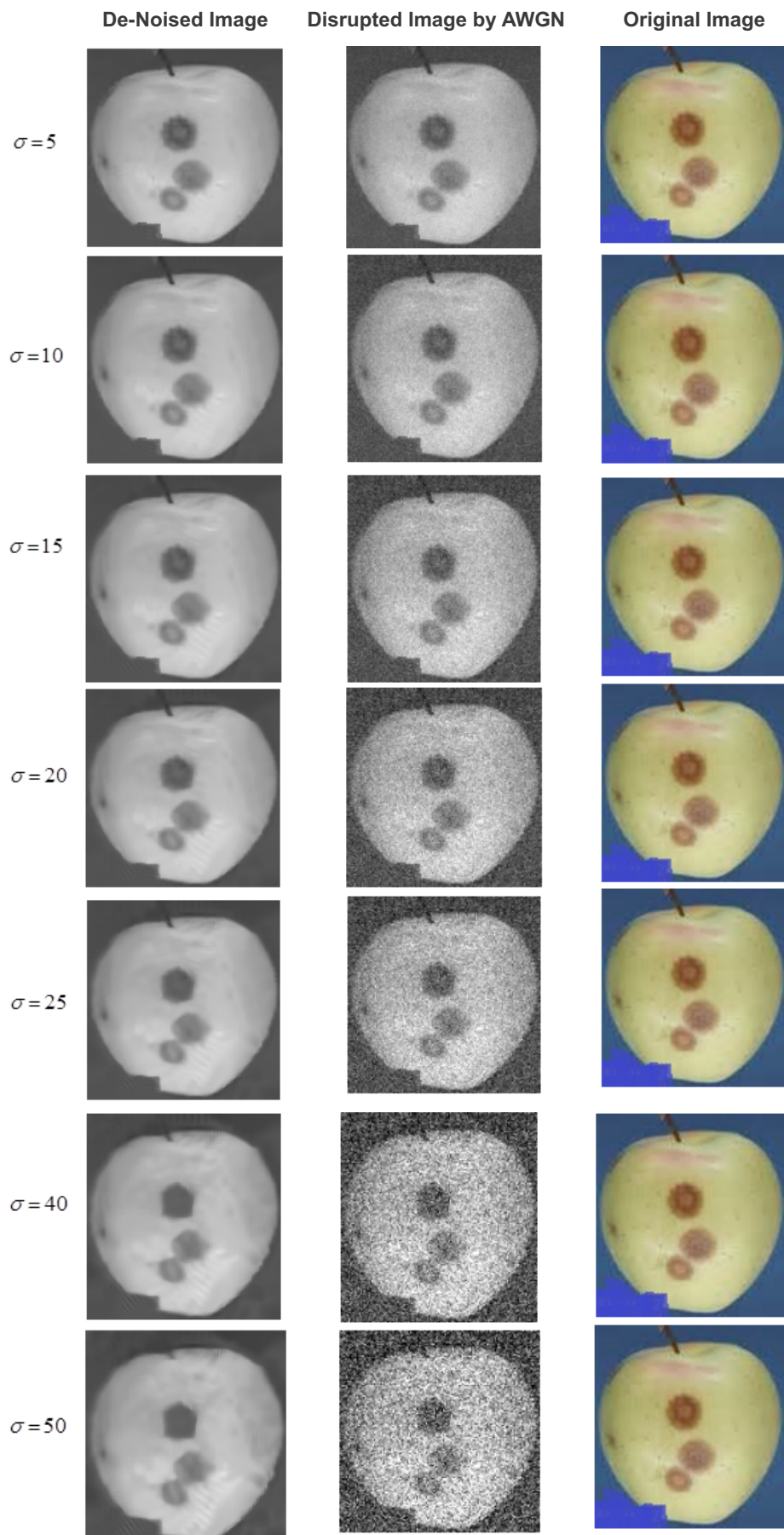


Figure 4: Results of applying the proposed De-Noising algorithm for different levels of standard deviation

Accurate Fruits Fault Detection in Agricultural Products / Saberhari

Table 1: Quantitative amounts of PSNR achieved by applying the presented De-Noising algorithm and comparing it with other methods

PGPCA	PID	Proposed
PSNR ($\sigma=5$)		
39.09	39.08	39.39
PSNR ($\sigma=10$)		
35.09	35.65	35.92
PSNR ($\sigma=15$)		
32.90	33.79	34.02
PSNR ($\sigma=25$)		
29.67	31.36	31.56
PSNR ($\sigma=40$)		
26.65	28.88	29.16
PSNR ($\sigma=50$)		
25.40	27.66	27.99

Table 2: Quantitative amounts of SSIM achieved by applying the presented De-Noising algorithm and comparing it with other methods

PGPCA	PID	Proposed
SSIM ($\sigma=5$)		
0.94899	0.95686	0.95772
SSIM ($\sigma=10$)		
0.8732	0.9232	0.92352
SSIM ($\sigma=15$)		
32.90	0.89424	0.89562
SSIM ($\sigma=25$)		
0.80685	0.83709	0.843
SSIM ($\sigma=40$)		
0.59105	0.7538	0.77505
SSIM ($\sigma=50$)		
0.53284	0.70451	0.73687

$$SMF = \frac{A_{segment} \cap A_{actual}}{A_{segment} \cup A_{actual}} \quad (11)$$

where $A_{segment}$ and A_{actual} are binary versions of segmented and actual images. For SMF parameter we have:

- If SMF=100%, we have full matching of images,

- If SMF > 50%, segmentation result is acceptable, and

- If SMF < 50%, segmentation result is weak.

Concordance correlation (P_c): this criterion determines the concordance between actual and segmented images. This criterion is applied to evaluate reproducibility of presented segmentation algorithms.

Accurate Fruits Fault Detection in Agricultural Products / Saberhari

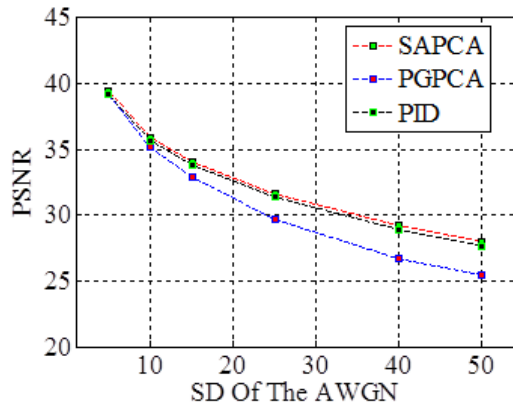


Figure 5: PSNR versus different levels of standard deviation of AWGN

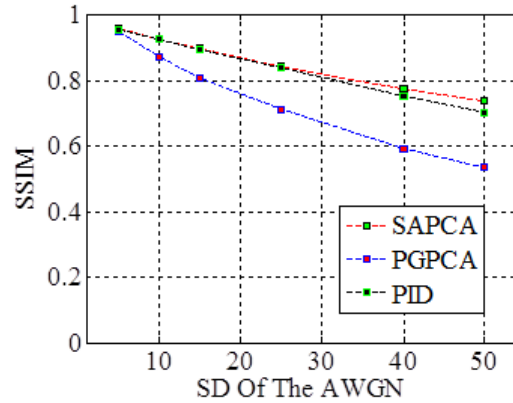


Figure 6: SSIM versus different levels of standard deviation of AWGN

P_c is defined as (Lehmussola *et al.*, 2006):

$$P_c(A, B) = \frac{2 S_A S_B r}{S_A^2 + S_B^2 + (\bar{A} - \bar{B})^2} \quad (12)$$

where A and B are two samples, \bar{A} and \bar{B} are the average amounts, S_A and S_B standard deviation of samples. The higher amount of P_c leads to the better the performance of the algorithm.

In figure 7, results of applying our algorithm

and also *Otsu* and *FCM* segmentation methods in fault identification of fruit images are compared. To assess the stability of the proposed algorithm in dealing with noise, fruit image have been destroyed with additive white Gaussian noise with the signal to noise ratio of 1, 3, 5, 7 and 9 (dB). In Tables 3 and 4, amounts of *SMF* and P_c are given for the proposed algorithm, *Otsu* segmentation and *FCM* methods. As seen, by increasing signal to noise ratio,

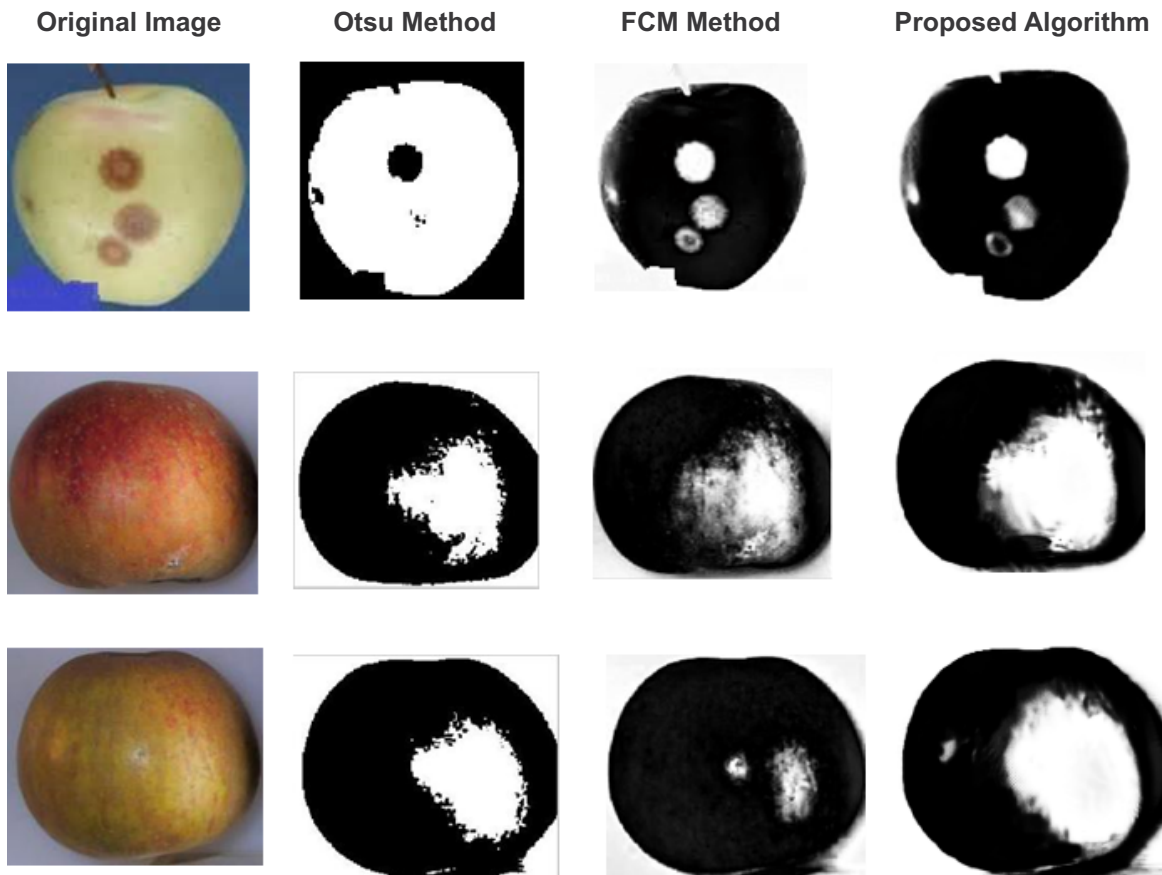


Figure 7: Results of performing the presented algorithm and comparing it with other methods in fruit images

Accurate Fruits Fault Detection in Agricultural Products / Saberhari

Table 3: Quantitative amounts of SMF achieved by applying the presented algorithm and comparing it with other methods (SD indicates the standard deviation)

SNR	Otsu	FCM	Proposed
1	78.2	81.2	92.6
3	78.9	86.6	93.4
5	82.2	87.1	95.2
7	86.1	89.9	97.4
9	89.6	92.5	98.3
	SD=4.8389	SD=4.2253	SD=2.4641

Table 4: Quantitative amounts of P_c achieved by applying the presented algorithm and comparing it with other methods (SD indicates standard deviation)

SNR	Otsu	FCM	Proposed
1	78.2	81.2	92.6
3	78.9	86.6	93.4
5	82.2	87.1	95.2
7	86.1	89.9	97.4
9	89.6	92.5	98.3
	SD=4.8389	SD=4.2253	SD=2.4641

SMF mount in the presented algorithm increases. For instance, by choosing SNR value equal to 7, SMF parameter in the presented algorithm improves by factor of 1.13 and 1.08 in comparison to Otsu and FCM, respectively. This shows that the proposed algorithm has good stability against noise.

CONCLUSION

A new segmentation algorithm has been proposed in this paper to detect faults in the fruits. The algorithm is consisted of three steps. First, to eliminate the background noise, we have used the combination of BM3D and PCA model. Then, we have performed our new compression approach to compress the de-noised image. This leads to increase the execution speed. Finally, the modified version of fuzzy-C means algorithm has been utilized to classify the pixels into foreground and background regions. Simulation results showed that the accuracy of the proposed algorithm is reached to 98.3% compared to other methods. One of the major advantages of our algorithm is its high speed characteristic which results in reduction of the run process. This leads to implementation of the hardware architecture of this algorithm to design an on-line fruit fault embedded identifier system. The other advantage is its stability rel-

ative to different levels of noise sources. As we have calculated, our proposed algorithm has the highest amounts of PSNR and SSIM parameters. Segmentation of different kinds of fruits with different skin colors is one of our major works for future.

ACKNOWLEDGEMENT

The author would like to acknowledge M.S. Alireza Farrokhinia for his guidance to improve the language of the manuscript. I also thank the anonymous reviewers of the paper for their valuable comments and suggestions.

REFERENCES

- 1- Abbot, J.A. (1999). Quality Measurement of fruits and vegetables. *Postharvest Biology and Technology*, 15, 207-225.
- 2- Ahmed, M.N., Yamany, S.M., Mohamed, N., & Farag, A. (2002). A modified fuzzy c-means algorithm for bias field estimation and segmentation of MRI data. *IEEE Transactions on Medical Imaging*, 21, 193-199.
- 3- Arumugam, N., Mohamed Arshad, F., Chiew, E., & Mohamed, Z. (2011). Determinates of fresh fruits and vegetables (FFV) farmers participation in contrast farming in Peninsular Malaysia. *International Journal of Agricultural Management and Development*, 1(2), 65-71.
- 4- Bezdek, J.C. (1987). Pattern recognition with

- fuzzy objective function algorithms. New York/ London, UK, Plenum.
- 5- Brosnan, T., & Sun, D.W. (2002). Inspection and grading of agriculture and food products by computer vision system-A reviews, *Computer and Electronic in Agriculture*. 36, 193-213.
- 6- Charles, D., Salmon, J., & Dalalyam, A. (2011). Image denoising with patch based PCA: local versus global. In Jesse Hoey, Stephen McKenna and Emanuele Trucco, *Proceedings of the British Machine Vision Conference*, pages 25.1-25.10. BMVA Press.
- 7- Dabov, K., Foi, A., Katkovnik, V., & Egiazarian, K. (2009). BM3D image denoising with shape-adaptive principle component analysis. *PROC. workshop on signal processing with adaptive sparse structured presentations (SPARS'09)*.
- 8- Foi, A., Katkovnik, V., & Egiazarian, K. (2007). Pointwise shape-adaptive DCT for high-quality denoising and deblocking of grayscale and color images. *IEEE Transactions on Image Processing*. 16, 1395-1411.
- 9- Graves, M., & Batchelor, B. (2003). *Machine vision for the inspection of Natural products*. London, Springer.
- 10- Halls, L., Evans, S., & Nott, K. (1998). Measurement of textural changes of food by MRI relaxometry. *Magnetic Resonance Imaging*, 16, 485-492.
- 11- Hills, B. (1995). Food processing and MRI perspective. *Trends in Food Science and Technology*. 6, 111-117.
- 12- Izadbakhshi, M., & Javadikia, H. (2014). Application of hybrid feed-forward neural network (ffnn)-genetic algorithm for predicting evaporation in storage dam reservoirs. *Agricultural Communications*, 2, 57-62.
- 13- Knaus, C., & Zwicker, M. (2014). Progressive image denoising. *IEEE Transactions on Image Processing*, 23, 3114-3125.
- 14- Lehmussola, A., Ruusuvoori, P., & Yli-Harja, O. (2006). Evaluating the performance of microarray segmentation algorithms. *Bioinformatics*, 22(23), 2910-2917.
- 15- Linker, R., Cohen, O., & Naor, A. (2012). Determination of the number of green apples in RGB images recorded in orchards. *Computers and Electronics in Agriculture*, 81, 45-57.
- 16- Malamas, E.N., Petrakis, E.G.M., Zervakis, M., Petit, L., & Legat, J.D. (2003). A survey on industrial vision systems, applications and tools. *Image and Vision Computing*, 21, 171-188.
- 17- Mizushima, A., & R. Lu. (2013). An image segmentation method for apple sorting and grading using support vector machine and Otsu's method. *Computers and Electronics in Agriculture*, 94, 29-37.
- 18- Moradi, G., Shamsi, M., Sedaghi, M. H., & Alsharif, M.R. (2011, April). Fruit defect detection from color images using ACM and MFCM algorithms. *International Conference on Electronic Devices, Systems and Applications (ICEDSA)*, 2011 International Conference on (pp. 182-186). IEEE.
- 19- Moradi, G., Shamsi, M., Sedaaghi, M.H. Moradi, S., & Alsharif, M. R. (2012). Apple defect detection using statistical histogram based EM algorithm. *19th Iranian Conference on Electrical Engineering (ICEE)*.
- 20- Payne, A.B. Walsh, K.B., Subedi, P.P., & Jarvis, D. (2013). Estimation of mango crop yield using image analysis- Segmentation method. *Computers and Electronics in Agriculture*, 91, 57-64.
- 21- Rakun, J., Stajanko, D., & Zazula, D. (2011). Detecting fruits in natural scenes by using spatial-frequency based texture analysis and multiview geometry. *Computers and Electronics in Agriculture*, 76, 80-88.
- 22- Romano, G. Argyropoulos, D., Nagle, M., Khan, M.T., & Muller, J. (2012). Combination of digital images and laser light to predict moisture content and color of bell pepper simultaneously during drying. *Journal of Food Engineering*. 119, 438-448.
- 23- Saberkari, H., & Shamsi, M. (2012). Comparison of different algorithms for ECG signal compression based on transfer coding. *IEEE Symposium on Industrial Electronics and Applications (ISIEA 2012)*, 23-26.
- 24- Saberkari, H., Bahrami, S., Shamsi, M., Amoshahy, M.J., Badri Ghavifekr, H., & Sedaaghi, M.H. (2015). Fully automated complementary DNA microarray segmentation using a novel fuzzy-based algorithm. *Journal of Medical Signals and Sensors*, 5(3), 182-191.
- 25- Huynh-Thu, Q., & Ghanbari, M. (2008). Scope of validity of PSNR in image/video quality assessment. *Electronics Letters*, 44(13), 800-801.

How to cite this article:

Saberkari, H. (2016). Accurate fruits fault detection in agricultural products using an efficient algorithm.

International Journal of Agricultural Management and Development, 6(2), 181-192.

URL: http://ijamad.iaurasht.ac.ir/article_523364_1e3fd111ae7252ac9e78b912e568ef69.pdf

